

Communication

# Comparison of Catalytic Activity of Chromium–Benzenedicarboxylate Metal–Organic Framework Based on Various Synthetic Approach

Tian Zhao \* , Hexin Zhu and Ming Dong

School of Packaging and Materials Engineering, Hunan University of Technology, Zhuzhou 412007, China; culaisett@126.com (H.Z.); dongming666@126.com (M.D.)

\* Correspondence: tian\_zhao@hut.edu.cn; Tel.: +86 13117538886

Received: 26 February 2020; Accepted: 9 March 2020; Published: 10 March 2020



**Abstract:** MIL-101(Cr), as a prototypical mesoporous metal–organic framework (MOF), can be facially prepared by involving different modulators to fit various demands. In this paper, a range of MIL-101(Cr) products were prepared under similar conditions. It was found that one of the additives, phenylphosphonic acid (PPOA), could give a stable hierarchical structure material. Compared to other MIL-101(Cr)s, though hierarchical MIL-101(Cr) showed less porosity, it gave a better catalytic performance in the oxidation of indene and 1-dodecene.

**Keywords:** hierarchical MIL-101(Cr); modulators; better catalytic activity

## 1. Introduction

MIL-101(Cr), found by the group of G. Férey, manifested ultrahigh porosity (BET surface area allowed to  $4100 \pm 200 \text{ m}^2/\text{g}$ , BET = Brunauer Emmett Teller) and excellent hydrolytic/chemical stability [1] which received great attention [2,3] and extended to various applications [4–6]

Nowadays, the most common synthetic procedure was employing hydrofluoric acid, as a so-called mineralizing agent, to improve its crystallinity and porosity [1]. However, hydrofluoric acid (HF), as a toxicant, is not suitable for large-scale synthesis, and the work-up procedures are quite tedious [1,4]. Thus, in order to avoid the using of HF in the synthesis, the researchers also developed other synthetic approaches by using other additives instead of HF. These substitutes could be alkalis acids or salts. For instance, NaOH was used to replace HF in the synthesis, which gave a nano-sized product with relatively good porosity ( $S_{\text{BET}} > 3200 \text{ m}^2/\text{g}$ ) and fairly good yield ( $\sim 40 \%$ ), which revealed a higher  $\text{CO}_2$  uptake [7,8]. Tetramethylammonium hydroxide (TMAOH) was used to improve the properties of MIL-101(Cr), which produced high quality material with repeatable BET surface areas and showed excellent performance in catalysis or water adsorption [9,10]. Furthermore, the particle sizes of MIL-101(Cr) could be changed from 19 to 84 nm by adding a suitable amount of monocarboxylic acid [11]. Acetic acid and nitric acid promoted either porosity or yield of MIL-101(Cr)—the difference is that the former possessed nano-sized particles [12] while the latter gave large and micron-scale crystals [13]. Adding lithium/potassium acetate was proven efficient in obtaining highly porous MIL-101(Cr) whose BET surface area could measure up to  $3400 \text{ m}^2/\text{g}$  [14].

Hierarchically porous metal–organic frameworks (HP-MOFs) state increasing interest due to their ascendancy performance compared to their parent MOFs in catalysis [15–17], large molecules in adsorption/separation [18,19], sensors [20] and energy storage applications [21,22], etc. Due to its high thermal stability and harsh synthesis temperature ( $220 \text{ }^\circ\text{C}$  usually), the directly synthesis of hierarchical MIL-101(Cr) was hard to achieve. In the previous research, we developed a template-free hydrothermal method to prepared HP-MIL-101(Cr) with large mesopores of around 4–10 nm via employing

phenylphosphonic acid (PPOA) as an additive [23]. Additionally, the prepared HP-MIL-101(Cr) presented better catalytic activity in the oxidation of indene compare with additive-free MIL-101(Cr). However, the catalytic performance of HP-MIL-101(Cr) in other reactions, especially compared with highly porous MIL-101(Cr) via the addition of other modulators, was still lacking investigation. Herein, we systematically compared the properties of HP-MIL-101(Cr), such as structure, morphology and catalytic activity. All the MIL-101(Cr) samples were synthesized under similar conditions (220 °C, with the hydrothermal method in an autoclave; for details, please see the Experimental Section), but with different additives in the synthesis. The selected modulator, including phenylphosphonic acid (PPOA), nitric acid (HNO<sub>3</sub>), hydrofluoric acid (HF), sodium hydroxide (NaOH), Tetramethylammonium hydroxide (TMAOH) and acetic acid (HOAc), and the corresponding products were named as PPOA-MIL-101(Cr), HNO<sub>3</sub>-MIL-101(Cr), HF-MIL-101(Cr), NaOH-MIL-101(Cr), TMAOH-MIL-101(Cr) and HOAc-MIL-101(Cr), respectively. The analytic results revealed that, though PPOA-MIL-101(Cr) possessed the lowest BET surface area, it had the highest catalytic activity in the oxidation of indene and indene and 1-dodecene.

## 2. Results and Discussion

The modulators were not only affecting the surface areas of MIL-101(Cr)s, but also influenced the particle sizes of the products. Figure 1 clearly demonstrates the particle size difference of the MIL-101(Cr)s. According to the previous report, the MIL-101(Cr) without any additives possessed a relatively large particle size (300~400 nm) [8,12]. When adding additives in the synthesis, the particle sizes of MIL-101(Cr) would decrease in varying degrees, which depended on the type and amount of the additives. This is because the modulators would compress the framework extension of MOF in the synthesis procedure [24]. In most cases, the particle sizes can be simply recognized to fall in the range of 100~200 nm (Figure 1). The only exception was nitric acid; HNO<sub>3</sub> slowed the nucleation speed and, at a lower pH environment, would yield larger crystals of MOF [13,25]. Thus, the addition of modulators significantly affects the morphology of MIL-101(Cr) products.

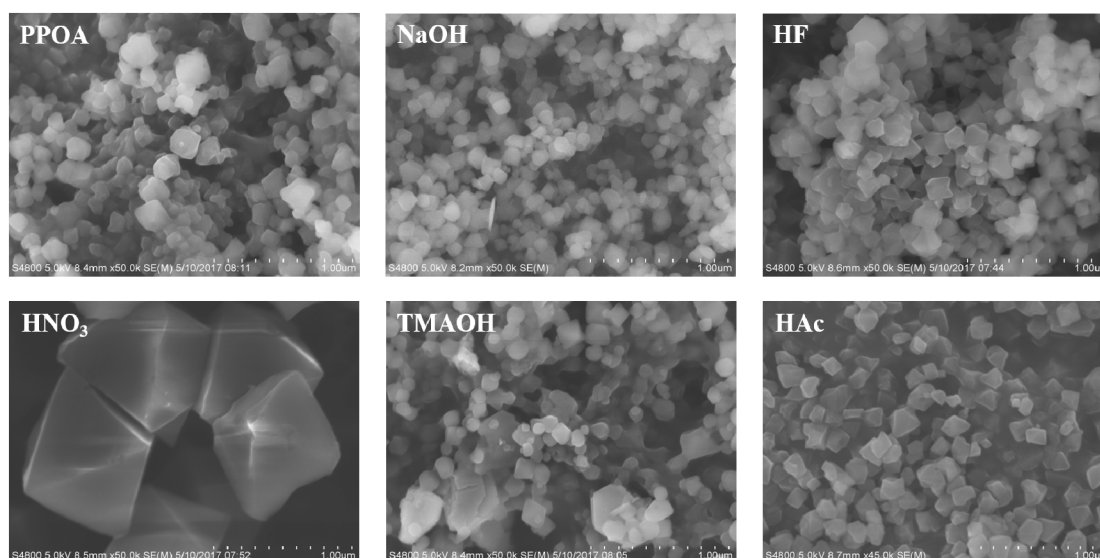


**Figure 1.** SEM images of MIL-101(Cr)s with various modulators in the synthesis, all the images with the same magnification and the scale bar is 1  $\mu\text{m}$ .

N<sub>2</sub> physical sorption isotherms of all MIL-101(Cr)s and their corresponding pore size distribution curves (PSDs) are displayed in Figure 2. Though all the MIL-101(Cr)s followed the same treatment procedure, the porosities demonstrated great difference (for details, please see Table 1). NaOH-MIL-101(Cr) possessed the highest BET surface area ( $S_{\text{BET}} > 4000 \text{ m}^2/\text{g}$ ) and the largest pore volume ( $2.01 \text{ cm}^3/\text{g}$ ), which may be attributed to the shift in the equilibrium of the formation

of MIL-101(Cr) that was caused by the increased pH value [7]. The second echelon involved HF-MIL-101(Cr) and HNO<sub>3</sub>-MIL-101(Cr), whose BET surface area exceeded 3000 m<sup>2</sup>/g. Although the use of HF in MIL-101(Cr) synthesis cannot reach the high BET surface area (> 4000 m<sup>2</sup>/g) as the original report described [1], HF-MIL-101(Cr) with a BET surface area of 3498 m<sup>2</sup>/g was also considered acceptable. HNO<sub>3</sub>-MIL-101(Cr) possessed not only a high BET surface area (3187 m<sup>2</sup>/g), but also revealed the highest yield (>80%), which was much larger than any other cases (around 50%, Table 1). Hence, the use of HNO<sub>3</sub> in MIL-101(Cr) was considered the best proposal for the large-scale synthesis of MIL-101(Cr) material [8,13]. Moreover, HOAc-MIL-101(Cr) and TMAOH-MIL-101(Cr) had fairly good porosity ( $S_{\text{BET}}$  was close to 3000 m<sup>2</sup>/g) and relatively small particle sizes, especially in the case of acetic acid; when its concentration reaches 3.5 mmol/mL, a nano-sized MIL-101(Cr) product with an average diameter of ~90 nm can be achieved [12].

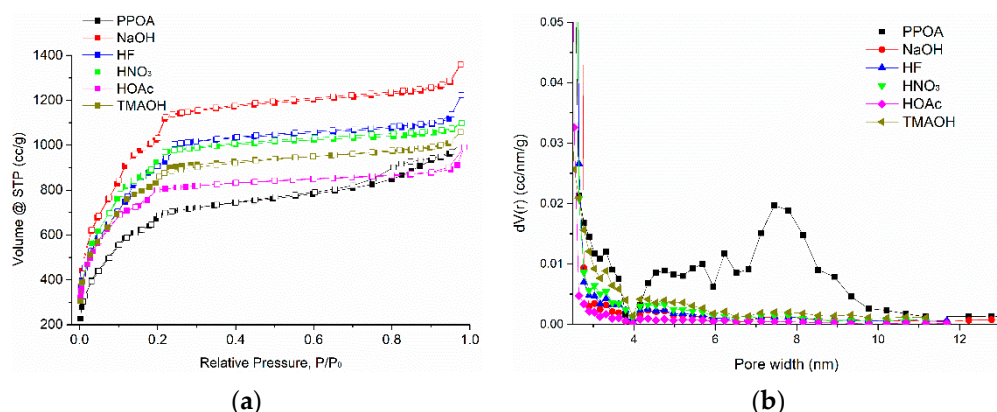


**Figure 2.** (a) Nitrogen adsorption-desorption isotherms of MIL-101(Cr)s, (b) and the corresponding pore size distribution curves (PSDs), which were calculated by the nonlocal-density functional theory (NL-DFT) model.

**Table 1.** The yield, surface area and pore volume of MIL-101(Cr) products with distinct modulators.

Sample	Yield (%) <sup>a</sup>	$S_{\text{BET}}$ (m <sup>2</sup> /g) <sup>b</sup>	$S_{\text{Langmuir}}$ (m <sup>2</sup> /g)	$V_{\text{pore}}$ (cm <sup>3</sup> /g) <sup>c</sup>
PPOA-MIL-101(Cr)	46	2329	3350	1.49
HF-MIL-101(Cr)	49	3498	4985	1.72
HNO <sub>3</sub> -MIL-101(Cr)	81	3187	4636	1.65
HOAc-MIL-101(Cr)	53	2894	3914	1.38
NaOH-MIL-101(Cr)	47	4065	5796	2.01
TMAOH-MIL-101(Cr)	51	2939	4245	1.55

<sup>a</sup> The Cr: bdc ratio is always 1:1, and the yield is based on Cr. <sup>b</sup>  $S_{\text{BET}}$  were determined in the pressure range  $0.05 < p/p_0 < 0.2$  from N<sub>2</sub> sorption isotherms at 77 K with an estimated standard deviation of  $\pm 50$  m<sup>2</sup>/g. <sup>c</sup> Obtained from N<sub>2</sub> sorption isotherm at 77 K ( $p/p_0 = 0.95$ ) for pores  $\leq 20$  nm.

Powder X-ray diffraction (PXRD) analysis disclosed that all the PXRD diffractograms of MIL-101(Cr)s matched the simulated PXRD pattern very well (Figure 3). Thus, the modulators we used here with suitable amounts did not affect the formation of MIL-101(Cr) products.

Compared to other MIL-101(Cr)s, PPOA-MIL-101(Cr) had the lowest  $S_{\text{BET}}$  of 2329 m<sup>2</sup>/g, but it showed a special hysteresis loop between the adsorption and desorption isotherms (Figure 2a), which was clearly different from the other samples. This character revealed the presence of larger mesopores, which indicated a hierarchical structure of PPOA-MIL-101(Cr) [23,26]. The pore size distributions of the MIL-101(Cr)s with the nonlocal-density functional theory (NL-DFT) method disclosed that PPOA-MIL-101(Cr) possessed mesopores with diameter around 4~10 nm, while the other MIL-101(Cr)s only had the natural pores of the framework (Figure 2b). Thus, it would be interesting to see the catalytic performance of these MIL-101(Cr)s.

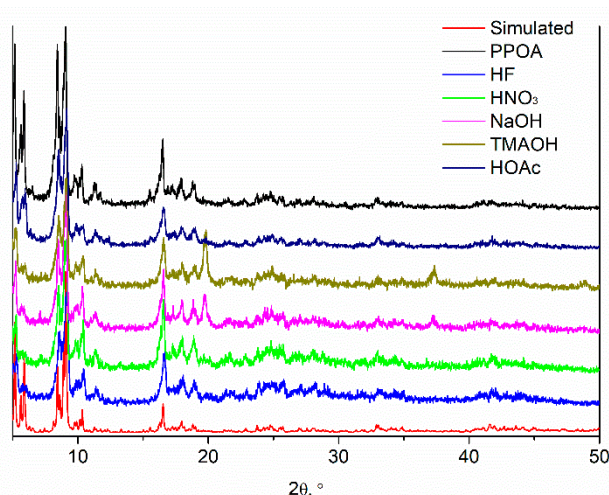


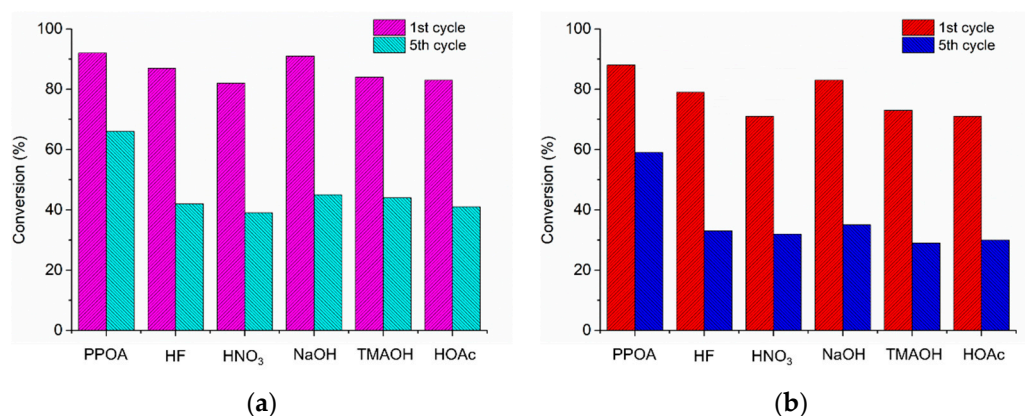
**Figure 3.** The powder X-ray diffraction (PXRD) diffractograms of MIL-101(Cr)s compared with simulated pattern.

As we knew, MIL-101(Cr) was an effective catalyst for the oxidation of indene and 1-dodecene [5,23]. The catalytic activities of the MIL-101(Cr)s are listed in Table 2. Moreover, for intuitive comparison, the columnar illustration of conversion of indene and 1-dodecene with the first run and the fifth run is presented in Figure 4. Obviously, PPOA-MIL-101(Cr) had the best catalytic activities among all MIL-101(Cr)s. In the first run, PPOA-MIL-101(Cr) showed the highest conversion for the oxidation of indene (92%) and 1-dodecene (88%), respectively. Additionally, the corresponding turnover frequency (TOF) value up to  $46 \text{ mmol}\cdot\text{g}^{-1}\cdot\text{h}^{-1}$  and  $8.8 \text{ mmol}\cdot\text{g}^{-1}\cdot\text{h}^{-1}$  (Table 2). Moreover, after five cycles, PPOA-MIL-101(Cr) still revealed a relatively good catalytic capability, the conversion of indene and 1-dodecene were 66% and 59%, respectively, while, for other samples, they also displayed a good catalytic performance at the first run (Table 2). This was especially the case for NaOH-MIL-101(Cr), whose conversion (91%) and TOF values ( $45.5 \text{ mmol}\cdot\text{g}^{-1}\cdot\text{h}^{-1}$ ) were very close to PPOA-MIL-101(Cr). However, after five cycles, all the other MIL-101(Cr)s without hierarchical porosity demonstrated a large decrease in conversion for both reactions. Furthermore, the conversion of PPOA-MIL-101(Cr) was over 20% higher than that of other MIL-101(Cr)s in both catalytic tests (Table 2). Thus, hierarchical MIL-101(Cr) (PPOA) indeed accelerated the diffusion rate and exposed more coordination in the metal sites of MIL-101(Cr), which eventually led to better catalytic performance in the oxidation of indene and 1-dodecene, though it had a lower BET surface area. Another point which needs to be noted is that TMAOH-MIL-101(Cr) and HOAc-MIL-101(Cr), which had relatively lower porosity, did not show the worst catalytic behavior (Table 2). On the contrary,  $\text{HNO}_3$ -MIL-101(Cr), which possessed relatively high porosity, exhibited the worst catalytic performance compared to other MIL-101(Cr)s, especially after five cycles (Table 2). This is because  $\text{HNO}_3$ -MIL-101(Cr) had much larger crystals than other MIL-101(Cr)s (Figure 1). In addition, larger particle size increased the difficulty for the external substrates, such as indene and 1-dodecene molecules, in accessing the internal activity sites of MIL-101(Cr), hence decreasing its catalytic activity.

**Table 2.** The conversion of indene and 1-dodecene by MIL-101(Cr) with different modulators.

Sample <sup>a</sup>	Conversion/TOF (mmol·g <sup>-1</sup> ·h <sup>-1</sup> ) (indene <sup>b</sup> , 1 <sup>st</sup> run)	Conversion (indene <sup>b</sup> , 5 <sup>th</sup> run)	Conversion/TOF (mmol·g <sup>-1</sup> ·h <sup>-1</sup> ) (1-dodecene <sup>b</sup> , 1 <sup>st</sup> run)	Conversion (1-dodecene <sup>b</sup> , 5 <sup>th</sup> run)
PPOA-MIL-101(Cr)	92%/46	66%	88%/8.8	59%
HF-MIL-101(Cr)	87%/43.5	42%	79%/7.9	33%
HNO <sub>3</sub> -MIL-101(Cr)	82%/41	39%	71%/7.1	32%
NaOH-MIL-101(Cr)	91%/45.5	45%	83%/8.3	35%
TMAOH-MIL-101(Cr)	84%/42	44%	73%/7.3	29%
HOAc-MIL-101(Cr)	83%/41.5	41%	71%/7.1	30%

<sup>a</sup> Sample was dried in the vacuum oven over night. <sup>b</sup> Mole ratio:(indene or 1-dodecene)/H<sub>2</sub>O<sub>2</sub> = 4/1, 70 °C, get 2-(carboxymethyl) benzoic acid (1 h) and undecanoic acid (5 h) respectively. <sup>c</sup> Turnover frequency (TOF) of the catalyst = (molar conversion of substrate)/(mass of MIL-101(Cr) × reaction time).

**Figure 4.** Comparison of the conversion of (a) indene and (b) 1-dodecene with MIL-101(Cr)s as catalysts for the first run and the fifth run.

### 3. Experimental Section

#### 3.1. The Preparation of MIL-101(Cr)s

The MIL-101(Cr)s were obtained with one equivalent of the additive based on Cr (except PPOA, which was 0.25 equivalently, with respect to Cr). A typical synthesis followed the consequent procedures. Cr(NO<sub>3</sub>)<sub>3</sub>·9H<sub>2</sub>O (400 mg, 1 mmol; Aladdin, Shanghai, China), terephthalic acid (166mg, 1 mmol; Aladdin, Shanghai, China) and the selected additive (1 mmol; PPOA is 0.25 mmol; Aladdin, Shanghai, China) were properly mixed in H<sub>2</sub>O (5 mL), which were placed in a Teflon liner in a hydrothermal autoclave (HTLAB, Shanghai, China). Then the autoclave was heated at 220 °C for 8 h and cooled afterwards, slowly, to ambient temperature.

All the cooled products were separated by centrifugation and treated with hot N,N-dimethylformamide (DMF, 80 °C, 15 mL; Sinopharm chemical reagent Co., Ltd., Beijing, China) for 1 h. This process was repeated once and then hot ethanol (15 mL, 60 °C; Sinopharm chemical reagent Co., Ltd., Beijing, China) was used to wash the products twice (for 1 h each). After centrifugation, the green products were carefully gathered and dried in a vacuum oven (120 °C, 1200 Pa, 2 h). All chemicals were purchased from commercial sources without any further treatments.

#### 3.2. Characterization

Powder X-ray diffraction (PXRD) measurements were conducted at room temperature (RT) via an Ultima IV instrument.

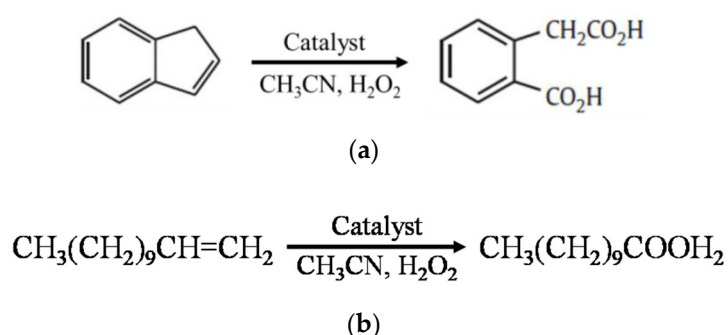
N<sub>2</sub>-sorption measurements were carried out in a NOVA-4000e instrument.

Scanning electron microscopy (SEM) characterizations were performed on a Nova NanoSEM230 instrument.

The conversion of reactants was analyzed via an Agilent Technologies 7890A GC system with capillary column at room temperature. The dodecane (1 mmol) was added as reference to determine the concentrations of the products.

### 3.3. Catalysis Reaction

The oxidation of indene and 1-dodecene: the catalyst (MIL-101(Cr)s, 10 mg), indene (0.5 mmol; Aladdin, Shanghai, China) or 1-dodecene (0.5 mmol; Aladdin, Shanghai, China) and acetonitrile (2 mL, Aladdin, Shanghai, China), was mixed in a tube and stirred for 10 min at 70 °C. Then, hydrogen peroxide solution (500  $\mu$ L, 30 wt%, 5 mmol; Aladdin, Shanghai, China) was added into the mixture and the timing of the reaction began. The catalytic products were monitored by gas chromatography (GC), and the reaction schemes were presented in Scheme 1.



**Scheme 1.** The schemes of oxidation reaction of (a) indene and (b) 1-dodecene.

## 4. Conclusions

In summary, we have exhibited the properties and catalytic performance of MIL-101(Cr) by involving different additives. Although PPOA-MIL-101(Cr) possessed the lowest porosity, it demonstrated the best catalytic activity and catalytic stability in the oxidation of indene and 1-dodecene, which can be attributed to its hierarchical structure. Moreover, the larger crystals decreased the diffusion rate of the external molecules to some extent and affected the catalytic capability of MIL-101(Cr). Thus, for a porous catalyst like MIL-101(Cr), the catalytic performance is not only determined by its porosity, but is also affected by its hierarchical structure and particle sizes.

**Author Contributions:** Conceptualization and methodology, T.Z.; formal analysis, H.Z. and M.D.; resources, M.D.; writing—original draft preparation, T.Z.; writing—review & editing, T.Z. and H.Z. All authors have read and agreed to the published version of the manuscript.

**Funding:** The work was supported by the National Natural Science Foundation of China (51802094), the Science and Technology Program of Hunan Province, China (2018RS3084), the Natural Science Foundation of Hunan Province (2018JJ3122) and the Scientific Research Project of Hunan Provincial Department of Education (18B294).

**Conflicts of Interest:** The authors declare no conflict of interest.

## References

- Férey, G.; Mellot-Draznieks, C.; Serre, C.; Millange, F.; Dutour, J.; Surble, S.; Margiolaki, I. A chromium terephthalate-based solid with unusually large pore volumes and surface area. *Science* **2005**, *309*, 2040–2042. [[CrossRef](#)] [[PubMed](#)]
- Bromberg, L.; Diao, Y.; Wu, H.; Speakman, S.A.; Hatton, T.A. Chromium(III) Terephthalate Metal Organic Framework (MIL-101): HF-Free Synthesis, Structure, Polyoxometalate Composites, and Catalytic Properties. *Chem. Mater.* **2012**, *24*, 1664–1675. [[CrossRef](#)]

3. Liu, K.; Zhang, S.; Hu, X.; Zhang, K.; Roy, A.; Yu, G. Understanding the Adsorption of PFOA on MIL-101(Cr)-Based Anionic-Exchange Metal-Organic Frameworks: Comparing DFT Calculations with Aqueous Sorption Experiments. *Environ. Sci. Technol.* **2015**, *49*, 8657–8665. [[CrossRef](#)] [[PubMed](#)]
4. Hong, D.-Y.; Hwang, Y.K.; Serre, C.; Férey, G.; Chang, J.-S. Porous Chromium Terephthalate MIL-101 with Coordinatively Unsaturated Sites: Surface Functionalization, Encapsulation, Sorption and Catalysis. *Adv. Funct. Mater.* **2009**, *19*, 1537–1552. [[CrossRef](#)]
5. Ying, J.; Herbst, A.; Xiao, Y.-X.; Wei, H.; Tian, G.; Li, Z.; Yang, X.-Y.; Su, B.-L.; Janiak, C. Nanocoating of Hydrophobic Mesoporous Silica around MIL-101Cr for Enhanced Catalytic Activity and Stability. *Inorg. Chem.* **2018**, *57*, 899–902. [[CrossRef](#)] [[PubMed](#)]
6. Wickenheisser, M.; Janiak, C. Hierarchical embedding of micro-mesoporous MIL-101(Cr) in macroporous poly(2-hydroxyethyl methacrylate) high internal phase emulsions with monolithic shape for vapor adsorption applications. *Micropor. Mesopor. Mater.* **2015**, *204*, 242–250. [[CrossRef](#)]
7. Khan, N.A.; Kang, I.J.; Seok, H.Y.; Jhung, S.H. Facile synthesis of nano-sized metal-organic frameworks, chromium-benzenedicarboxylate, MIL-101. *Chem. Eng. J.* **2011**, *166*, 1152–1157. [[CrossRef](#)]
8. Zhao, T.; Li, S.; Shen, L.; Wang, Y.; Yang, X.-Y. The sized controlled synthesis of MIL-101(Cr) with enhanced CO<sub>2</sub> adsorption property. *Inorg. Chem. Commun.* **2018**, *96*, 47–51. [[CrossRef](#)]
9. Herbst, A.; Khutia, A.; Janiak, C. Bronsted Instead of Lewis Acidity in Functionalized MIL-101Cr MOFs for Efficient Heterogeneous (nano-MOF) Catalysis in the Condensation Reaction of Aldehydes with Alcohols. *Inorg. Chem.* **2014**, *53*, 7319–7333. [[CrossRef](#)]
10. Wickenheisser, M.; Herbst, A.; Tannert, R.; Milow, B.; Janiak, C. Hierarchical MOF-xerogel monolith composites from embedding MIL-100(Fe,Cr) and MIL-101(Cr) in resorcinol-formaldehyde xerogels for water adsorption applications. *Micropor. Mesopor. Mater.* **2015**, *215*, 143–153. [[CrossRef](#)]
11. Jiang, D.; Burrows, A.D.; Edler, K.J. Size-controlled synthesis of MIL-101(Cr) nanoparticles with enhanced selectivity for CO<sub>2</sub> over N<sub>2</sub>. *CrystEngComm* **2011**, *13*, 6916–6919. [[CrossRef](#)]
12. Zhao, T.; Yang, L.; Feng, P.; Gruber, I.; Janiak, C.; Liu, Y. Facile synthesis of nano-sized MIL-101(Cr) with the addition of acetic acid. *Inorg. Chim. Acta* **2018**, *471*, 440–445. [[CrossRef](#)]
13. Zhao, T.; Jeremias, F.; Boldog, I.; Nguyen, B.; Henninger, S.K.; Janiak, C. High-yield, fluoride-free and large-scale synthesis of MIL-101(Cr). *Dalton Trans.* **2015**, *44*, 16791–16801. [[CrossRef](#)] [[PubMed](#)]
14. Zhou, J.; Liu, K.; Kong, C.; Chen, L. Acetate-assisted Synthesis of Chromium(III) Terephthalate and Its Gas Adsorption Properties. *Bull. Korean Chem. Soc.* **2013**, *34*, 1625–1631. [[CrossRef](#)]
15. Feng, L.; Yuan, S.; Li, J.-L.; Wang, K.-Y.; Day, G.S.; Zhang, P.; Wang, Y.; Zhou, H.-C. Uncovering Two Principles of Multivariate Hierarchical Metal–Organic Framework Synthesis via Retrosynthetic Design. *ACS Cent. Sci.* **2018**, *4*, 1719–1726. [[CrossRef](#)]
16. Jiao, L.; Wan, G.; Zhang, R.; Zhou, H.; Yu, S.-H.; Jiang, H.-L. From Metal-Organic Frameworks to Single-Atom Fe Implanted Ndoped Porous Carbons: Efficient Oxygen Reduction in Both Alkaline and Acidic Media. *Angew. Chem. Int. Ed.* **2018**, *57*, 1–6. [[CrossRef](#)]
17. Feng, L.; Yuan, S.; Zhang, L.-L.; Tan, K.; Li, J.-L.; Kirchon, A.; Liu, L.-M.; Zhang, P.; Han, Y.; Chabal, Y.J.; et al. Creating Hierarchical Pores by Controlled Linker Thermolysis in Multivariate Metal-Organic Frameworks. *J. Am. Chem. Soc.* **2018**, *140*, 2363–2372. [[CrossRef](#)]
18. Guan, H.-Y.; LeBlanc, R.J.; Xie, S.-Y.; Yue, Y. Recent progress in the syntheses of mesoporous metal-organic framework materials. *Coordin. Chem. Rev.* **2018**, *369*, 76–90. [[CrossRef](#)]
19. Zhu, L.; Zong, L.; Wu, X.; Li, M.; Wang, H.; You, J.; Li, C. Shapeable Fibrous Aerogels of Metal–Organic-Frameworks Templated with Nanocellulose for Rapid and Large-Capacity Adsorption. *ACS Nano* **2018**, *12*, 4462–4468. [[CrossRef](#)]
20. Wang, Z.; Liu, T.; Asif, M.; Yu, Y.; Wang, W.; Wang, H.; Xiao, F.; Liu, H. Rimelike Structure-Inspired Approach toward in Situ-Oriented Self-Assembly of Hierarchical Porous MOF Films as a Sweat Biosensor. *ACS Appl. Mater. Interfaces* **2018**, *10*, 27936–27946. [[CrossRef](#)]
21. Zhang, M.; Dai, Q.; Zheng, H.; Chen, M.; Dai, L. Novel MOF-Derived Co@N-C Bifunctional Catalysts for Highly Efficient Zn-Air Batteries and Water Splitting. *Adv. Mater.* **2018**, *30*, 1705431. [[CrossRef](#)] [[PubMed](#)]
22. Feng, D.; Lei, T.; Lukatskaya, M.R.; Park, J.; Huang, Z.; Lee, M.; Shaw, L.; Chen, S.; Yakovenko, A.A.; Kulkarni, A.; et al. Robust and conductive two-dimensional metal–organic frameworks with exceptionally high volumetric and areal capacitance. *Nat. Energy* **2018**, *3*, 30–36. [[CrossRef](#)]

23. Zhao, T.; Dong, M.; Yang, L.; Liu, Y. Synthesis of Stable Hierarchical MIL-101(Cr) with Enhanced Catalytic Activity in the Oxidation of Indene. *Catalysts* **2018**, *8*, 394. [[CrossRef](#)]
24. Hermes, S.; Witte, T.; Hikov, T.; Zacher, D.; Bahnmuller, S.; Langstein, G.; Huber, K.; Fischer, R. Trapping metal-organic framework nanocrystals: An in-situ time-resolved light scattering study on the crystal growth of MOF-5 in solution. *J. Am. Chem. Soc.* **2007**, *129*, 5324–5325. [[CrossRef](#)] [[PubMed](#)]
25. Xin, C.; Zhan, H.; Huang, X.; Li, H.; Zhao, N.; Xiao, F.; Wei, W.; Sun, Y. Effect of various alkaline agents on the size and morphology of nano-sized HKUST-1 for CO<sub>2</sub> adsorption. *RSC Adv.* **2015**, *5*, 27901–27911. [[CrossRef](#)]
26. Thommes, M.; Kaneko, K.; Neimark, A.V.; Olivier, J.P.; Rodriguez-Reinoso, F.; Rouquerol, J.; Sing, K.S.W. Physisorption of gases, with special reference to the evaluation of surface area and pore size distribution (IUPAC Technical Report). *Pure Appl. Chem.* **2015**, *87*, 1051–1069. [[CrossRef](#)]



© 2020 by the authors. Licensee MDPI, Basel, Switzerland. This article is an open access article distributed under the terms and conditions of the Creative Commons Attribution (CC BY) license (<http://creativecommons.org/licenses/by/4.0/>).